

OPEN

Possibility of Recycling SiO_x Particles Collected at Silicon Ingot Production Process as an Anode Material for Lithium Ion Batteries

Junghyun Kim¹, SoYeun Kim², Cheol-Min Yang² & Gyo Woo Lee¹

Recently, some studies have utilized silicon (Si) as an anode material of lithium ion battery by recycling Si from the slurry of wafer slicing dust. The filtration of Si particles condensed from Si vapors that were exhausted from the ingot growing furnace could propose another method of Si recycling. In this study, we investigated the possibility of using such collected silicon oxides (SiO_x) particles as an anode material. After collecting SiO_x particles, FE-SEM, TEM, EDS, XRD, XPS analysis, and charge/discharge test were carried out to investigate characteristics and usability of these particles. FE-SEM and FE-TEM images showed that these particles mainly consisted of spherical primary particles with a diameter of 10 nm or less. Agglomerates of these primary particles were larger than 300 nm in diameter. In TEM image and EDS analysis, crystalline particles were observed along with amorphous particles. As a result of XRD analysis, amorphous silica (SiO₂) and crystalline Si were observed. Charge/discharge tests were carried out to determine the feasibility of using these particles as an anode material for lithium ion batteries. A cycle efficiency of 40.6% was obtained in the test in which the total number of charge/discharge cycle was 100 under the condition of C-rate 0.2 for the first three times and C-rate 1.0 for the remaining 97 times. Results showed that these collected particles could be used as an anode material for lithium ion batteries.

Silicon (Si) has been widely used to fabricate semiconductors for electronic devices. It is utilized in the shape of a wafer made by melting raw polysilicon, growing in the form of a single crystal ingot, and then cutting the ingot thinly according to the purpose of use. The importance of renewable energy has been emphasized to reduce the consumption of fossil fuel. Si has also been used as a raw material for photovoltaic solar cells to utilize solar energy. With increasing need for solar cells due to the growth of photovoltaic cell market, demand for Si to produce wafer is steadily increasing^{1,2}.

However, a large amount of Si loss occurs in the slicing process using wire saws when a thin wafer is cut out from the cylindrical Si ingot. This kerf loss might increase the production cost of Si wafers. The resulting Si sludge adversely affects the environment, resulting in additional costs for the sludge treatment. In general, Si sludge from single-crystal ingot is consisted of kerf-loss crystalline Si and some impurities like lubricant oil and metal debris from the wire saw. When the sludge is recycled the impurities need to be removed through complex and expensive procedures^{3,4}. To reduce such loss of Si, several studies have tried to recycle Si from the sludge³⁻⁹. Wang *et al.*⁵ have recycled Si sludge to fabricate solar cells, and analyzed the performance of these cells. They reported that solar cells made from recycled Si could achieve a performance less than 2% compared to commercial solar cells, making it possible to use the recycled Si. Tsai^{6,7} has separated Si from impurities using electric force and particle weight. Tomono *et al.*⁸ have also studied the recycling of the produced sludge from a slicing process using diamond wires. Removal efficiencies of lubricant and metal impurities using acetone and acid solutions, respectively, were examined by thermal and elemental analyses. Sergiienko *et al.*⁹ have reported that Si sludge can be separated into Si and silicon carbide (SiC) by centrifugation and cyclone.

¹Division of Mechanical Design Engineering, Chonbuk National University, Jeonju, 54896, Republic of Korea.

²Institute of Advanced Composite Materials, Korea Institute of Science and Technology (KIST), Wanju, Jeollabuk-do, 55324, Republic of Korea. Correspondence and requests for materials should be addressed to G.L. (email: gwlee@jbnu.ac.kr)

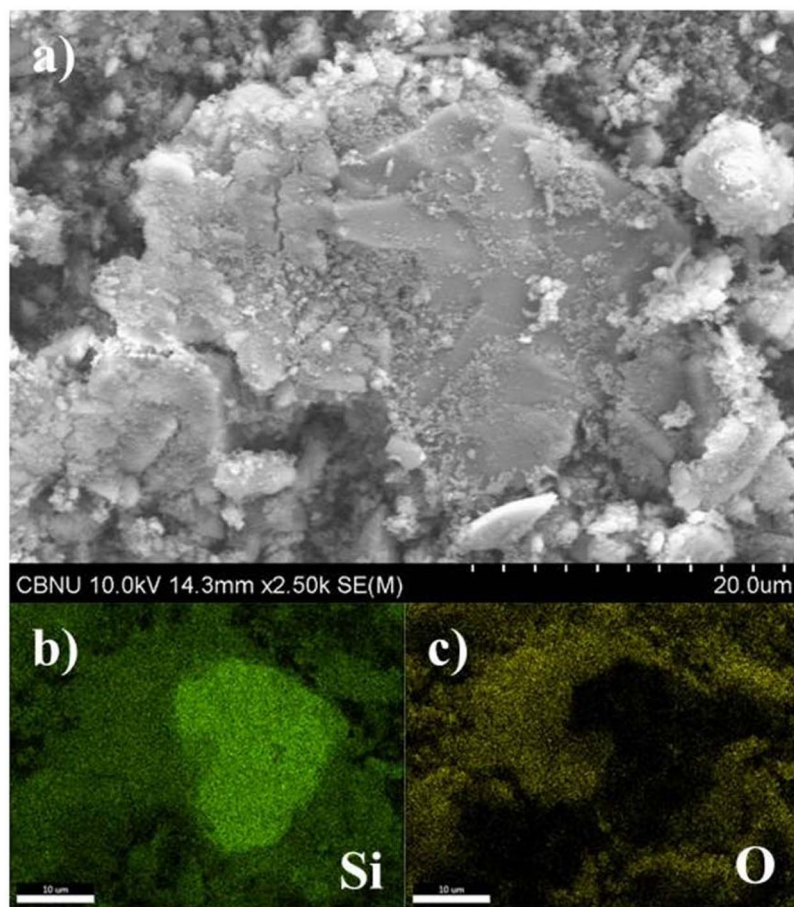


Figure 1. (a) FE-SEM image of the collected SiO_x particles, (b,c) EDS mappings of the collected SiO_x particles.

Various methods of secondary batteries have been explored in many researches throughout the years. Xie *et al.*¹⁰ reviewed the recent progress of Li-ion storage performances of various rhenium disulfide (ReS_2) electrodes, mainly focusing on the synthesis method, structures, the reaction mechanism, and the corresponding electrochemical performance. In 2018, Liao *et al.*¹¹ reported that the morphology, size and phase of the material (nano-sized niobium pentoxide) play a crucial role in its electrochemical performance, and discussed that the material has the great potential as a practical high-rate anode material for lithium-ion batteries. In the recent review paper, Wang *et al.*¹² summarized the synthesis strategies, common characterization techniques, and their important role in electrochemical lithium/sodium ions storage and capacitance properties of oxygen-defective metal oxides.

In this study, we investigated the possibility of recycling the silicon oxides (SiO_x) particles mixed with crystalline Si collected from Si vapors in the ingot growing process. It is expected that the coexistence of Si crystal and amorphous silica (SiO_2) particles could be helpful to achieve good electrochemical performances as an anode material for lithium ion batteries. Additionally, the proposed approach is based on a facile, green, and cost-effective process.

Results and Discussion

Particle characteristics. FE-SEM and EDS mapping images of the particles are shown in Fig. 1, including FE-SEM image of particles (Fig. 1a), Si element mapping (Fig. 1b), and O element mapping picture (Fig. 1c). Figure 1a has a scale bar of 20 μm and a particle size at the center is larger than 30 μm . Also, lots of nanometer scaled particles are seen around the large particles. FE-SEM image shows that these particles are a mixture of μm size particles and agglomerates of nm particles. EDS mapping photos in Fig. 1b and Fig. 1c show that regions of Si and O can be clearly distinguished. These mapping photos suggest that the particle larger than 30 μm in size in Fig. 1a might be Si crystal rather than SiO_x .

The averages and standard deviations of weight and atomic fractions for Si and O elements of the samples from the EDS analyses are as follows: 53.8 wt% (std. dev. = 8.5 wt%) and 40.3 at% (std. dev. = 8.7 at%) for Si and 46.2 wt% (std. dev. = 8.5 wt%) and 59.7 at% (std. dev. = 8.7 at%) for O element, respectively.

To investigate the composition of particles, XPS spectrum was obtained as shown in Fig. 2. In the XPS spectrum, Si and O elements were identified as in EDS analysis. In addition to these two elements, a small amount of C element was detected. It was originated from the graphitic heater in the ingot grower. Based on the results of

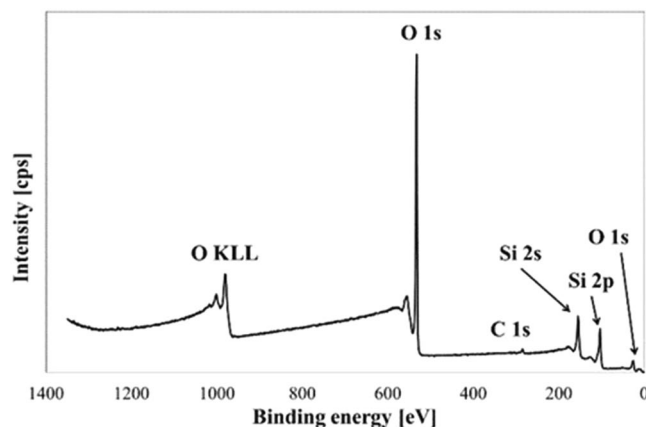


Figure 2. XPS spectra of SiO_x particles showing O, Si, and C elements.

EDS and XPS analyses we believed that the collected particles are mainly consisted of silicon oxides (SiO_x) and crystalline silicon (Si).

Figure 3 is TEM images of collected Si particles with crystalline structures. The scale bar is 100 nm in Fig. 3a and 5 nm in Fig. 3b. Agglomerates or aggregates of nanometer particles were approximately 300 nm in diameter. Figure 3b is an enlarged view of a rectangular portion seen at the central position of Fig. 3a. In the figure, the size of primary particles was less than 10 nm, and the lattice spacing was 0.31 nm. Crystalline particles could be found along with amorphous SiO_x particles.

Figure 4 is the XRD spectrum showing peaks of Si crystals, amorphous SiO_2 particles, and SiC. The broad peak at 2θ equals $20^\circ \sim 30^\circ$ on the left side of Fig. 4, showing the presence of amorphous SiO_2 . In case of larger than 30° for 2θ value several peaks confirm the presence of crystalline Si and SiC^{13–16}. When the SiO_x particles were used as an anode material, it was known through the result of the previous study that the higher the Si crystal content, the higher the charge/discharge capacity¹⁷. In their article, Takezawa *et al.*¹⁷ showed that the values of charge and discharge capacities were decreased with increasing values of x in SiO_x . On the basis of this literature and the XRD analysis we believe that it is quite possible to use the collected SiO_x powder as an anode materials of the lithium ion battery.

Figure 5 shows particle size distribution of collected particles. The distribution is bimodal with a group of nm sized particles and a group of μm sized particles. This could explain the μm sized particles shown in FE-SEM photographs and lots of agglomerated nm sized particles found around the μm sized particles. The mean sizes of the nm size group on the left and the μm size one on the right were 322.9 nm and 17.9 μm , with standard deviations of 40.7 nm and 3.5 μm , respectively. The specific surface area and average pore size of the particles measured by BET and BJH analyses were 184.4 m^2/g and 7.4 nm, respectively. FE-SEM image, the specific surface area, and the pore size suggested that tens of nanometer particles aggregated to form larger particles with diameter of approximately 300 nm and agglomerates of larger particles formed tens of micrometer sized particles.

These collected particles were identified as SiO_x particles mixed with crystalline Si through several analyses. When Si is used as an anode material for a lithium ion battery, crystalline Si is advantageous in terms of the capacity of the battery. There have been some attempts to utilize amorphous SiO_x particles because of disadvantages caused by the expansion and contraction of crystalline Si particles occurred during charging and discharging process¹⁸. In this view, proper mixing of these two types of particles (Si crystal and amorphous SiO_2) could be helpful to achieve good electrochemical performance when they are used as an anode material for lithium ion batteries.

Electrochemical property. Figure 6a shows the galvanostatic charge (Li^+ insertion) and discharge (Li^+ extraction) profiles of SiO_x anodes in the voltage range of 0.05 to 2.0 V (vs. Li/Li^+) at room temperature. As a result of the charge/discharge test, the initial charging capacity was 1572.8 mAh/g and the initial discharging capacity was 456.3 mAh/g.

According to the differential capacity plots for the SiO_x electrodes Fig. 6b, a broad peak is visible at ~ 0.8 V, which is mainly associated with the SEI layer formation on the surface of the SiO_x particles during the first charge. When the potential reaches ~ 0.25 V vs Li/Li^+ , Si begins to react with Li^+ , resulting two delithiation peaks at ~ 0.3 and 0.45 V vs Li/Li^+ , which are characteristics for the lithiation reactions of amorphous Li_xSi .

Figure 6c is a graph showing results of charge/discharge tests up to 100 cycles of the fabricated coin cell. The upper line of the graph shows coulombic efficiency change which means the ratio of the discharge capacity to the charge capacity. Lines at the bottom of the graph show change of charge and discharge capacity according to charge/discharge cycle. The battery capacity maintenance efficiency up to 100 cycles was 40.6% of the initial discharge capacity. This was lower than the average battery capacity retention efficiency (about 70%) of coin cells using modified Si as an anode material^{13–16}. The coulombic efficiency was 29.0% at the first charge/discharge and close to 100% after the 5th cycle. It is necessary to increase the initial coulombic efficiency through modification of particles.

The reason why the initial coulombic efficiency was low during charging and discharging was due to reaction of Si and electrolyte. In this reaction, a layer called SEI was formed on the Si surface. During the reaction, Li^+ was lost and the capacity was reduced. When SEI was formed, the reaction was terminated and Li^+ was used in the

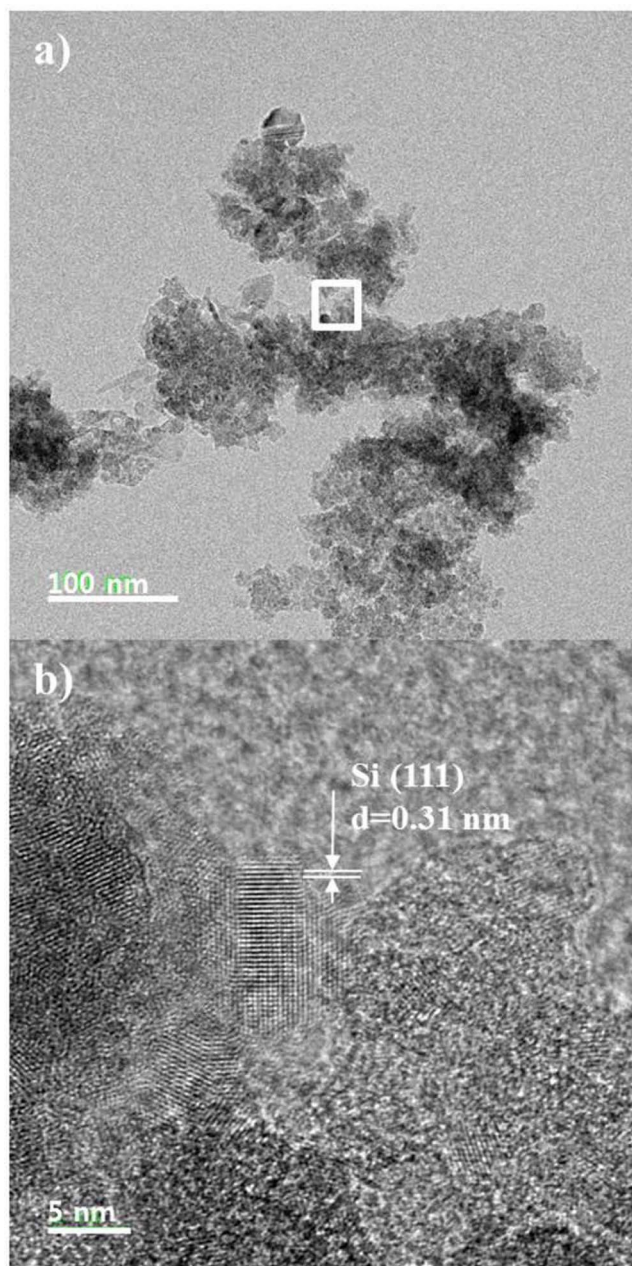


Figure 3. TEM images showing aggregated nanometer sized particles (a) and crystalline structures of particles with high magnification (b).

charge and discharge processes to maintain a coulombic efficiency of about 99%. However, if SEI cracks, a new SEI is created, resulting in lower efficiency^{18–20}. Based on charge/discharge test results, we believe that, if accompanied with surface modification, SiO_x particles collected from Si vapors in the ingot growing process could be utilized as an anode material of lithium ion battery.

Summary and Conclusion

The purpose of this study was to investigate the possibility of using recycled SiO_x particles as an anode material of a lithium ion battery. FE-SEM, EDS, TEM, XRD, PSA, BET and XPS analyses were done on SiO_x particles collected at the vapor exhaust duct of the ingot growing furnace. In addition, a half coin cell was prepared using these collected particles as an anode material and electrical characteristics of the cell were measured through charge/discharge test. Through these analyses, it was confirmed that the collected particles were SiO_x particles mixed with crystalline Si and amorphous SiO₂. These particles were distributed in two groups with average sizes of 322.9 nm and 17.9 μm. The specific surface area was 184.4 m²/g and the average pore size was 7.4 nm. In the charge/discharge test, the battery capacity maintenance efficiency was 40.6% compared to the initial discharge amount after up to 100 cycles and the coulombic efficiency was more than 99% after 5 cycles.

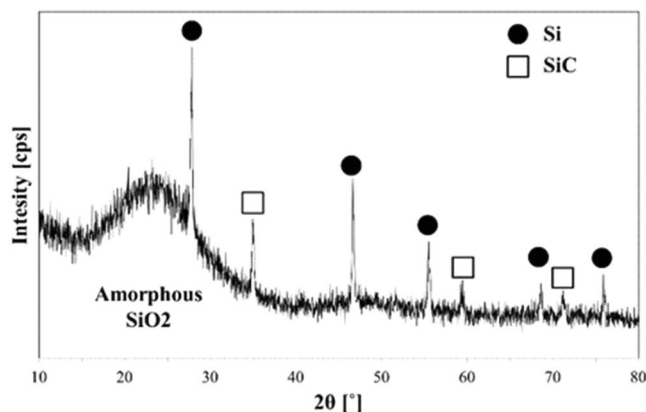


Figure 4. XRD peaks showing Si and SiC crystalline and amorphous SiO₂.

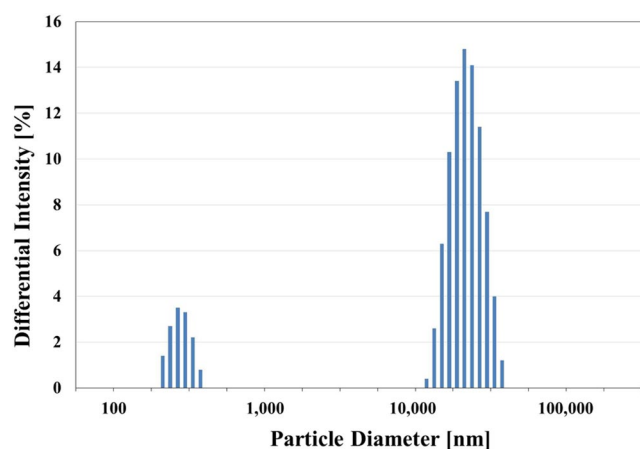


Figure 5. Particle size distribution showing a bimodal shape with mode values of 322.9 nm and 17.9 μm .

This study showed that the recycling SiO_x particles exhausted from the Si ingot grower is environmentally friendly and economical. Results also showed that these collected particles could be used as an anode material for lithium ion batteries.

Experimental Details

Collection of Si particles. Si particles were collected at a single crystal Si ingot grower made by S-Tech Co. Ltd. (Model SS1). The grower is currently operated by M company, one of domestic Si ingot producers in South Korea. The filtration system used for collecting Si particles was manufactured by H & D Co. Ltd. It is cylindrical in shape with an outer diameter of 558 mm, a length of 1315 mm, and a thickness of 8.5 mm. The filter installed for collecting particles was made by 3GS Co. Ltd. It has 10 mm thick glass fiber material and pores of 30 to 40 μm in diameter. The filter has 50 wrinkles with an inner diameter of 224 mm, an outer diameter of 359 mm, and a length of 535 mm. Details of particle collection were described in a previous work²¹.

Characterization of collected particles. To determine particle shape and compositions, field-emission scanning electron microscopy (FE-SEM) images were obtained and energy dispersive spectrometer (EDS) analysis was performed, respectively (SU-70, HITACHI). Brunauer-Emmett-Teller (BET) and Barrett-Joyner-Halenda (BJH) analyses from N₂ adsorption isotherms (77 K) measured using volumetric equipment were performed to confirm the specific surface area and pore size distribution of particles, respectively (ASAP2010, Micromeritics). Particle size analysis (PSA) was also performed to know the particle size distribution of particles (UPA-150, Microtrac). Cs-corrected field emission transmission electron microscopy (FE-TEM) analysis was also performed to confirm the crystal structure of particles (JEM-ARM-200F, JEOL). X-ray diffraction (XRD, MAX-2500, RIGAKU) and X-ray photoelectron spectroscopy (XPS, K-Alpha XPS System, Thermo Fisher Scientific) were used to observe crystalline structures.

Measurement of electrochemical property. A half-coin cell (CR 2032) was fabricated to check the possibility of using these collected Si particles as an anode material of the lithium ion secondary battery. Electrode was prepared by mixing three components [active material: binder (35 wt% PAA, Aldrich): conductive agent (Super P, Fisher Scientific) = 8: 1: 1 by weight] to make a slurry which was then applied to copper foil and dried

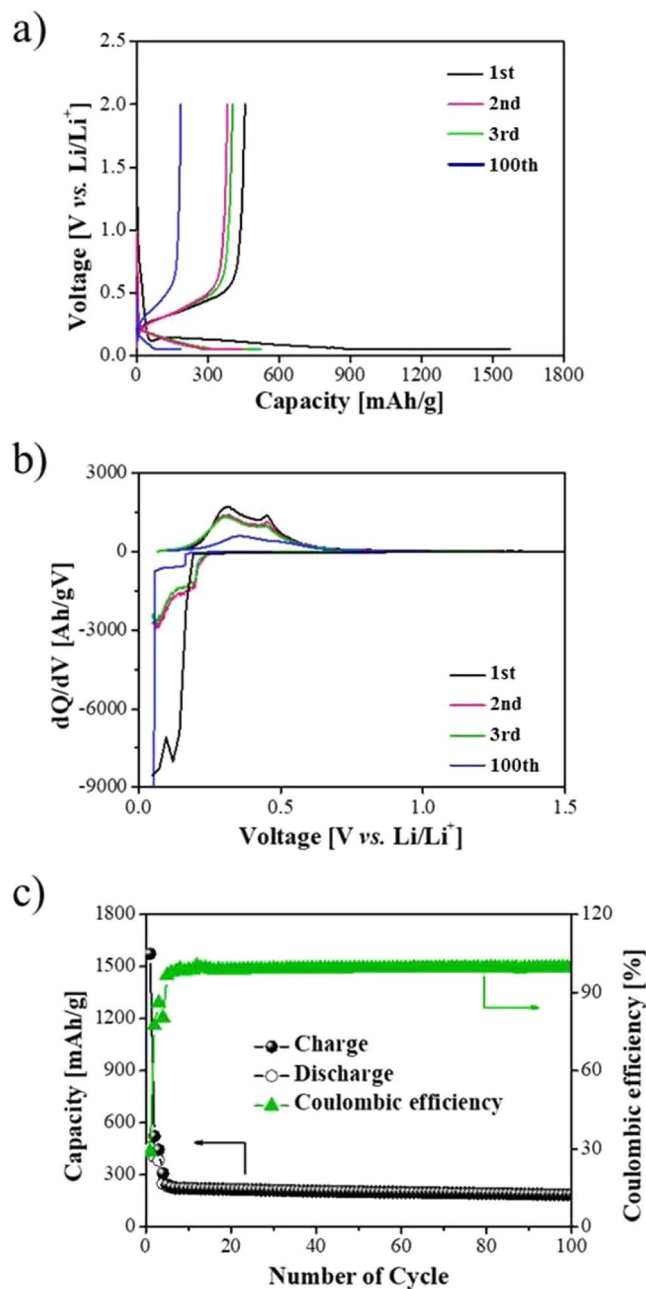


Figure 6. Electrochemical performance of SiO_x anode. (a) Galvanostatic charge and discharge profiles in the 1st, 2nd, 3rd, and 100th cycles. (b) Differential capacity vs. cell potential curves. (c) Cycle performance and coulombic efficiency of the half coin cell from 1 to 100 charge/discharge cycles.

at 80 °C for 6 hours. The painted copper foil was squeezed using a roll press and dried under vacuum at 120 °C for 12 hours. After that, circular electrode plates (15 mm in diameter, according to coin cell size) were made from the painted and completely dried copper foil using a punching machine. The electrolyte solution was 1 M LiPF₆ (Aldrich) in which ethylene carbonate (EC) and diethyl carbonate (DEC) were mixed at the same volume. WBCS3000Le32 tester (WonA Tech Co.) was used for charge/discharge test of the fabricated battery. Test conditions were set to 0.2 C rate for forming solid electrolyte interphase (SEI) up to the initial 3 cycles. Then 1.0 C rate was maintained for the following 97 cycles. The cut off condition was 0.05 to 2 V. It was the same for all 100 cycles.

References

1. Woditsch, P. & Koch, W. Solar grade silicon feedstock supply for PV industry. *Sol. Energy Mater. Sol. Cells* **72**, 11–26 (2002).
2. Saga, T. Advances in crystalline silicon solar cell technology for industrial mass production. *NPG Asia Mater.* **2**, 96–102 (2010).
3. Drouiche, N. *et al.* Recovery of solar grade silicon from kerf loss slurry waste. *Renew. Sustain. Energy Rev.* **32**, 936–943 (2014).
4. Drouiche, N. *et al.* Hidden values in kerf slurry waste recovery of high purity silicon. *Renew. Sustain. Energy Rev.* **52**, 393–399 (2015).
5. Wang, T. Y. *et al.* Recovery of silicon from kerf loss slurry waste for photovoltaic applications. *Prog. Photovoltaics Res. Appl.* **17**, 155–163 (2009).

6. Tsai, T. H. Modified sedimentation system for improving separation of silicon and silicon carbide in recycling of sawing waste. *Sep. Purif. Technol.* **78**, 16–20 (2011).
7. Tsai, T. H. Silicon sawing waste treatment by electrophoresis and gravitational settling. *J. Hazard. Mater.* **189**, 526–530 (2011).
8. Tomono, K. *et al.* Recycling of kerf loss silicon derived from diamond-wire saw cutting process by chemical approach. *Sep. Purif. Technol.* **120**, 304–309 (2013).
9. Sergiienko, S. A., Pogorelov, B. V. & Daniliuk, V. B. Silicon and silicon carbide powders recycling technology from wire-saw cutting waste in slicing process of silicon ingots. *Sep. Purif. Technol.* **133**, 16–21 (2014).
10. Xie, X., Mao, M., Qi, S. & Ma, J. ReS₂-Based electrode materials for alkali-metal ion batteries. *CrystEngComm* **21**, 3755–3769 (2019).
11. Liao, J. *et al.* Controlling the morphology, size and phase of Nb₂O₅ crystals for high electrochemical performance. *Chinese Chem. Lett.* **29**, 1785–1790 (2018).
12. Wang, L., Xie, X., Dinh, K. N., Yan, Q. & Ma, J. Synthesis, characterizations, and utilization of oxygen-deficient metal oxides for lithium/sodium-ion batteries and supercapacitors. *Coord. Chem. Rev.* **397**, 138–167 (2019).
13. Jang, H. D. *et al.* Aerosol-Assisted Extraction of Silicon Nanoparticles from Wafer Slicing Waste for Lithium Ion Batteries. *Sci. Rep.* **5**, 1–5 (2015).
14. Kim, S. K. *et al.* One-Step Formation of Silicon-Graphene Composites from Silicon Sludge Waste and Graphene Oxide via Aerosol Process for Lithium Ion Batteries. *Sci. Rep.* **6**, 1–8 (2016).
15. Bao, Q., Huang, Y. H., Lan, C. K., Chen, B. H. & Duh, J. G. Scalable Upcycling Silicon from Waste Slicing Sludge for High-performance Lithium-ion Battery Anodes. *Electrochim. Acta* **173**, 82–90 (2015).
16. Chou, C. Y., Kuo, J. R. & Yen, S. C. Silicon-Based Composite Negative Electrode Prepared from Recycled Silicon-Slicing Slurries and Lignin/Lignocellulose for Li-Ion Cells. *ACS Sustain. Chem. Eng.* **6**, 4759–4766 (2018).
17. Takezawa, H., Iwamoto, K., Ito, S. & Yoshizawa, H. Electrochemical behaviors of nonstoichiometric silicon suboxides (SiO_x) film prepared by reactive evaporation for lithium rechargeable batteries. *J. Power Sources* **244**, 149–157 (2013).
18. Chen, T., Wu, J., Zhang, Q. & Su, X. Recent advancement of SiO_x-based anodes for lithium-ion batteries. *J. Power Sources* **363**, 126–144 (2017).
19. Ashuri, M., He, Q. & Shaw, L. L. Silicon as a potential anode material for Li-ion batteries: Where size, geometry and structure matter. *Nanoscale* **8**, 74–103 (2016).
20. Feng, K. *et al.* Silicon-Based Anodes for Lithium-Ion Batteries: From Fundamentals to Practical Applications. *Small* **14** (2018).
21. Kim, J., Ahn, J., Kang, H. Y. & Lee, G. W. Collection of Silicone Nanoparticles in Ingot Growing Process and Analysis of Particle Characteristics. *Key Eng. Mater.* **777**, 145–149 (2018).

Acknowledgements

This work (Grant No. 0504805) was supported by Business for Cooperative R&D between Industry, Academy, and Research Institute funded by Korea Small and Medium Business Administration in 2017.

Author Contributions

J. Kim designed and prepared the material, conducted the experiments, and wrote the paper; S.Y. Kim and C.-M. Yang conducted experiments related to the electrochemical performance, and analyzed the result; G.W. Lee designed the study, analyzed the result and revised the paper.

Additional Information

Competing Interests: The authors declare no competing interests.

Publisher's note Springer Nature remains neutral with regard to jurisdictional claims in published maps and institutional affiliations.



Open Access This article is licensed under a Creative Commons Attribution 4.0 International License, which permits use, sharing, adaptation, distribution and reproduction in any medium or format, as long as you give appropriate credit to the original author(s) and the source, provide a link to the Creative Commons license, and indicate if changes were made. The images or other third party material in this article are included in the article's Creative Commons license, unless indicated otherwise in a credit line to the material. If material is not included in the article's Creative Commons license and your intended use is not permitted by statutory regulation or exceeds the permitted use, you will need to obtain permission directly from the copyright holder. To view a copy of this license, visit <http://creativecommons.org/licenses/by/4.0/>.

© The Author(s) 2019